Pharm Res (2012) 29:739–755
DOI 10.1007/s11095-011-0599-y

RESEARCH PAPER

Novel 1-indanone Thiosemicarbazone Antiviral Candidates: Aqueous Solubilization and Physical Stabilization by Means of Cyclodextrins

Romina J. Glisoni • Diego A. Chiappetta • Albertina G. Moglioni • Alejandro Sosnik

Received: 5 April 2011 / Accepted: 20 September 2011 / Published online: 6 October 2011

ABSTRACT

Purpose To investigate cyclodextrin-mediated solubilization and physical stabilization of novel 1-indanone thiosemicarbazone (TSC) candidate drugs that display extremely high self-aggregation and precipitation tendency in water.

Methods TSC/CD complexes were produced by co-solvent method, and TSC/CD phase-solubility diagrams were obtained by plotting TSC concentration as a function of increasing CD concentration. Size, size distribution, and zeta-potential of the different TSC/CD complexes and aggregates were fully characterized by dynamic light scattering. The morphology of the structures was visualized by atomic force microscopy.

Results Results indicated the formation of Type A inclusion complexes; the solubility of different TSCs was enhanced up to 215 times. The study of physical stability revealed that, as opposed to free TSCs that self-aggregate, crystallize, and precipitate in water very rapidly, complexed TSCs remain in solution for at least 1 week. On the other hand, a gradual size growth was observed. This phenomenon stemmed from the self-aggregation of the TSC/CD complex.

Conclusions 1-indanone TSC/CD inclusion complexes improved aqueous solubility and physical stability of these new drug candidates and constitute a promising technological approach towards evaluation of their activity against the viruses hepatitis B and C.

KEY WORDS 1-indanone thiosemicarbazone antiviral candidates · inclusion complexes · native and modified cyclodextrins · self-assembly · water-solubilization

INTRODUCTION

Drug self-assembly is a phenomenon whereby poorly-water soluble amphiphilic drug molecules self-associate spontaneously in water above a critical concentration (1). This behavior was reported for amphotericin B (AmB) (2), penicillins (3), non-steroidal anti-inflammatories (4), antidepressants (5), antipsychotics (6), non-nucleoside reverse transcriptase inhibitors (7), phthalocyanines (8) and (E)-resveratrol (9). The most important drawback, when this phenomenon takes place in biological media, relies on the partial or total loss of the biological activity owing to the more limited ability of the aggregates to surpass biological barriers (10). Moreover, drugs aggregates may display increased toxicity *in vivo*; e.g., AmB aggregates are nephrotoxic (2).

The potential therapeutic application of thiosemicarbazones (TSCs) emerged with the description of their *in vitro* activity against *Mycobacterium tuberculosis* (11). Since then,

Electronic supplementary material The online version of this article (doi:10.1007/s11095-011-0599-y) contains supplementary material, which is available to authorized users.

R. J. Glisoni · D. A. Chiappetta · A. Sosnik (✉)
The Group of Biomaterials & Nanotechnology for Improved Medicines (BIONIMED)
Department of Pharmaceutical Technology
Faculty of Pharmacy & Biochemistry, University of Buenos Aires
956 Junín St., 6th Floor
Buenos Aires CP1113, Argentina
e-mail: alesosnik@gmail.com

R. J. Glisoni · D. A. Chiappetta · A. G. Moglioni · A. Sosnik
National Science Research Council (CONICET)
Buenos Aires, Argentina

A. G. Moglioni
Department of Pharmacology, Faculty of Pharmacy & Biochemistry
University of Buenos Aires
Buenos Aires, Argentina

TSCs displaying antineoplastic (12), antibacterial (13), antifungal (14), antiprotozoal (15) and antiviral (16) activity have been reported. Moglioni *et al.* designed novel 1-indanone TSC candidate drugs that have shown *in vitro* activity against viruses, bacteria and fungi (17–20). For example, 5,6-dimethoxy-1-indanone TSC (Fig. 1a) displayed a 7-fold increase in the selectivity index against the virus of the bovine viral diarrhea (BVDV), a surrogate model of the hepatitis C virus (HCV), with respect to ribavirin (17,20); ribavirin is the first-choice anti-HCV agent combined with pegylated interferon-alpha. However, TSCs display extremely low aqueous solubility and precipitate rapidly in the culture medium, leading to unreliable antiviral half maximal inhibitory concentration (IC_{50}) data (17). In a recent study, we reported for the first time on the self-aggregation behavior of TSCs in water (21). In this context, the investigation of an appropriate drug carrier that improves the aqueous solubility of TSCs and prevents their self-aggregation remains a key stage towards the comprehensive evaluation of their antiviral activity in hepatitis B (HBV) and HCV cell constructs.

Cyclodextrins (CDs) are macrocyclic oligosaccharides that combine a hydrophobic nano-sized cavity with a hydrophilic surface (Fig. 1b) (22,23). The cavity enables the partial or total incorporation of lipophilic molecules. Thus, CDs are extensively used to increase the water solubility and bioavailability of lipophilic drugs. Two types of complexes can coexist: (i) inclusion and (ii) non-inclusion complexes (24,25). The CD complexation of these drugs may also prevent their self-aggregation into a crystal lattice and their precipitation (9,26,27). On the other hand, native and chemically modified CDs display an intrinsic self-assembly tendency in water that leads to the generation of physically stable nano-aggregates (28). Drug/CD complexes may also self-aggregate (29), this phenomenon being often driven by the guest molecule, especially when it self-aggregates (30). On the other hand, the aggregates of drug/CD inclusion complexes can contribute to improve the solubility and physical stability of the drug in water (30,31). Depending on the properties of the CD, the self-aggregation of the complex in water can result in the appearance of opalescence (31). For example, hydrophobic drug/gamma-CD (γ-CD) complexes show turbidity upon increasing γ-CD concentration, while solutions of the 2-hydroxypropyl gamma-CD (HPγ-CD) remain transparent (32). The addition of relatively small amounts of chemically-modified CDs to solutions of unmodified CDs can minimize the appearance of opalescence but does not prevent their self-aggregation (31,32). Due to their good biocompatibility and their approval by the US-FDA and the European Medicines Agency, CDs have become broadly used pharmaceutical excipients.

The goal of the present work was to increase the water solubility and prevent the self-aggregation, crystallization and precipitation of a series of potentially antiviral 1-indanone TSCs by means of CD complexation. The molecular parameters that govern the capacity of native and chemically-modified CDs to host the different TSCs were primarily investigated. Then, the work was focused on 5,6-dimethoxy-1-indanone TSC, the derivative that has shown the most promising preliminary antiviral activity.

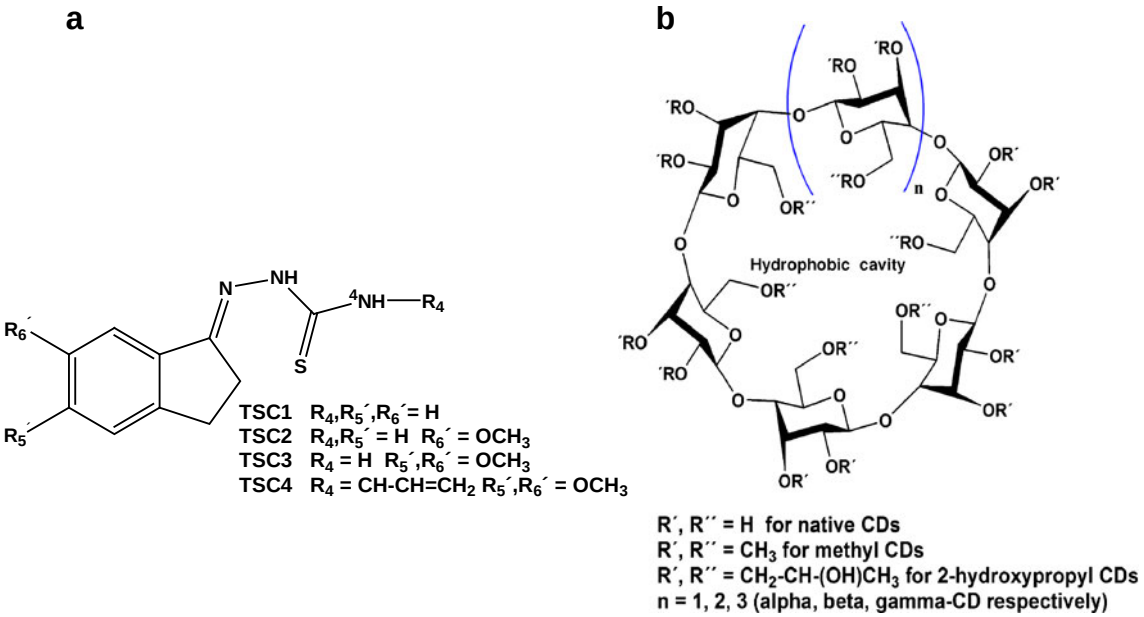

Fig. 1 Chemical structure of the different (**a**) thiosemicarbazones and (**b**) cyclodextrins included in the present work.

MATERIALS AND METHODS

Materials

1-indanone TSC, 6-methoxy-1-indanone TSC, 5,6-dimethoxy-1-indanone TSC and 5,6-dimethoxy-1-indanone N4-allyl TSC are named TSC1, TSC2, TSC3 and TSC4, respectively (Fig. 1a). They were synthetized and purified as depicted elsewhere (21). Alpha-CD (Cavamax® W_6; α-CD), gamma-CD (Cavamax® W_8; γ-CD), 2-hydroxypropyl beta-CD (Cavasol® W_7 HP; HPβ-CD; molar substitution, MS, per anhydro glucose unit of 0.65; average molecular weight, M_W of 1400 Da) and methyl beta-CD (Cavasol® W_7 M; Mβ-CD, MS of 1.75, M_W of 1310 Da) were from Wacker-Chemie GmbH (Germany) and a gift of SAFER S.A.C.I.F (Argentina). 2-Hydroxypropyl γ-CD (Cavasol® W_8 HP; HPγ-CD, MS of 0.60, M_W of 1575 Da) was from Wacker-Chemie and provided by ISP Technologies (Argentina). The structure of the CDs used in this work is presented in Fig. 1b. All the solvents were of analytical grade and used without further purification. Phase solubility and stability studies, DLS analysis and microscopy were conducted employing MilliQ water (Simplicity UV Water Purification System, Millipore, USA).

Critical Aggregation Concentration (CAC) of Native and Modified CDs

The *CAC* of the different CDs was determined to establish the concentration at which aggregates are formed. Derived Count Rate (DCR) measurements were carried out by means of Dynamic Light Scattering (DLS) using a Zetasizer Nano-ZS (Malvern Instruments, UK) at scattering angle of 173°. The Nano-ZS contains a 4 mW He-Ne laser operating at a wavelength of 633 nm, a digital correlator ZEN3600, and a Non-Invasive Back Scatter (NIBS®) technology. CD aqueous solutions of increasing concentration were prepared in MilliQ water at 25°C and filtered (0.45 μm, GE nitrocellulose mixed esters membrane plastic syringe filters, Osmonics Inc., USA). The intensity of the scattered light expressed in kilo counts per second (Kcps, DCR) was plotted as a function of the CD concentration (mM) (33). The intersection between the two lines was established as the *CAC*.

Preparation of TSC/CD Inclusion Complexes

The preparation of TSC/CD inclusion complexes was carried out by the cosolvent method, in triplicate. Depending on the CD, polar organic solvent mixtures or water/polar organic solvent mixtures were used (34). HPβ-CD, HPγ-CD, and Mβ-CD were dissolved in methanol at the desired concentration and the corresponding TSC (in slight excess) was dissolved in methanol:acetone (1:1) or chloroform:acetone (1:1) (for TSC3). Then, both solutions were thoroughly mixed over 15 min under magnetic stirring, at 25°C. In the case of α-CD and γ-CD complexes, CDs were dissolved in a minimum volume of water and mixed well with the organic solution. The solvent was removed under vacuum using a rotary evaporator (15 min, 70–90°C, Fbr®, Decalab S.R.L, Argentina). White powders were re-dissolved in MilliQ water, the volume being in accordance with the final CD concentration. Solutions were magnetically stirred (30 min, 25°C) to solubilize the complex and finally filtered (0.45 μm, GE nitrocellulose mixed esters membrane plastic syringe filters). This is the commonly used technique to remove insoluble drug residues after the CD complexation and a prerequisite for DLS measurements. In general, the initial size of the CD aggregates and TSC/CD complex aggregates was smaller than 450 nm (see below). In the case of higher CD concentrations that resulted in larger structures, the pressure applied during filtration ensured the disassembly of the aggregates and the appropriate filtration. Thus, the amount of TSC/CD retained by the filter was negligible. This was confirmed by filtering the same sample with filters of 1.2 μm, where no diference in the TSC concentration was observed. TSC/CD complex solutions displayed pH values between 6.5 and 7.5. Phase diagrams were prepared by plotting the TSC concentration in the system *versus* the final CD concentration. The TSC concentration in the complex was determined by UV spectrophotometry (see below) (21). From these data, a solubility factor (F) was calculated according to Eq. 1

$$F = S_{CD}/S_0 \quad (1)$$

where S_{CD} and S_0 are the TSC solubility in the CD and pure water, respectively. $F_{3\%}$ and F_{max} are defined as the solubility factors obtained in (i) 3% w/v CD and (ii) a system of maximum CD concentration. While the former represents a usually cyto and biocompatible CD concentration, the latter indicates the maximum TSC solubility attainable with a specific CD and could be relevant for the development of a pharmaceutical formulation.

Preparation of Freeze-Dried TSC/CD Inclusion Complexes

To characterize the different TSC/CD complexes, the filtrates obtained above (5 mL) were frozen at −80°C (24 h) and freeze-dried in a chamber freeze-dryer (Lyophilizer L05, F.i.c, Scientific Instrumental Manufacturing, Argentina) at a condenser temperature of −40°C and 30 μbar pressure. TSC/CD physical mixtures (PMs, control) were prepared by thoroughly mixing freeze-dried CD and pristine TSC. PMs were employed to evaluate the intrinsic

sensitivity of a technique to detect the TSC when included in the complex and contained a TSC/CD weight ratio identical to that of the complex.

TSCs were quantified by UV spectrophotometry (CARY [1E] UV-visible Spectrophotometer Varian, USA), according to a technique described elsewhere (21). Calibration curves of the different TSCs were built with water:dimethyl sulfoxide (DMSO) (98:2) solutions in the 7.5–75.0 μM concentration range. Absorbances were measured at 312, 324, 329 and 330 nm for TSC1, TSC2, TSC3 and TSC4, respectively (21). Those TSC/CD systems that became opalescent in water (e.g., α-CD and γ-CD) were conveniently diluted in DMSO to enable UV analysis (21).

Analysis of Residual Organic Solvents

To adjust the experimental conditions and ensure the complete removal of organic solvents during rotaevaporation, "drug-free" HPβ-CD systems were prepared as described above, though the incorporation of the TSC into the methanol:acetone or chloroform:acetone mixture was obviated. After solvent evaporation, samples (0.6 g) were re-suspended in dichloromethane (CH_2Cl_2, 7 mL) and left overnight to enable the extraction of any solvent traces; HPβ-CD is insoluble in CH_2Cl_2. Samples were centrifuged (10 min, 5000 rpm), filtered (0.45 μm) to remove the insoluble CD and the supernatant (1 μL) was analyzed by gas chromatography (GC, Shimadzu GC-9A instrument with FID detection, Japan). The separation was carried out on a capillary column Heliflex AT-1 (length: 60 m, i.d.: 0.25 mm, film thickness 0.25 μm, Alltech Associates Inc., USA) with He as carrier at a flow of 1 kg/cm^2. The temperature of the injector and the oven was 250°C and 40°C, respectively. A mixture of CH_2Cl_2 and MeOH (1 μL) was injected to verify that both elution peaks were resolved (0.81 and 0.70 min, respectively). MeOH displays the highest boiling temperature of all the organic solvents employed in the preparation process. Thus, the content of residual solvents was expressed as total residual MeOH. A calibration curve with increasing MeOH concentrations in CH_2Cl_2 (0.5–3.0% v/v) and fixed internal standard of cyclohexane (retention time: 1.33 min) was plotted. Analyses were performed in triplicate. Chromatograms were analized by Win PCChromXY software (Faculty of Pharmacy and Biochemistry, University of Buenos Aires, Argentina).

Determination of TSC/CD Phase-Solubility Profiles

Phase solubility profiles of the different TSCs in the different CDs were obtained by plotting TSC concentration (M) *versus* CD concentration (M). Mean apparent stability constants ($k_{1:1}$), expressed in M^{-1}, were calculated according to the phase solubility method of Higuchi and Connors (35) employing Eq. 2:

$$k_{1:1} = \text{slope}/[S_0(1 - \text{slope})] \quad (2)$$

where S_0 is the intrinsic solubility of TSCs in water treated under identical conditions though, in the absence of CD. The condition for the employment of this equation to calculate the $k_{1:1}$ is that the slope is smaller than the unity; slopes were calculated from the linear portion of the curve, regardless of the phase diagram pattern (22).

The mean complexation efficiency (CE) was calculated according to Eq. 3, from the slope of linear phase-solubility diagrams (36):

$$CE = [TSC \times CD]/[CD] = S_0 \times k_{1:1} = \text{slope}/(1 - \text{slope}) \quad (3)$$

where [TSC×CD] is the total TSC solubility in presence of CD and [CD] is the total CD concentration in moles per liter.

Characterization of TSC/CD Inclusion Complexes

Attenuated Total Reflectance/Fourier Transform-Infrared Spectroscopy (ATR/FT-IR)

The TSC/CD interaction was initially studied by ATR/FT-IR (Perkin Elmer Spectrum BX FT-IR Spectrometer, Perkin Elmer Inc., USA) in the range between 4000 and 500 cm^{-1} (15 scans, spectral resolution of 4.0 cm^{-1}). Solid samples (pure TSCs, native and modified CDs, TSC/CD inclusion complexes and TSC/CD PMs) were mounted on the ATR crystal-metal plate. PMs were prepared by mixing TSC and CD in a weight ratio identical to that in the complex. The signals of pure TSC and CD were compared to those of TSC/CD and PM. FT-IR spectra were obtained using the Spectrum v.5.3.1 software (Perkin Elmer Inc., UK).

Size, Size Distribution and Z-potential Analysis

The hydrodynamic size (D_h), size distribution (polydispersity index, PDI) and zeta-potential (Z-potential) of the different complexes were assayed by DLS (see above). The temperature was controlled at 25°C (all the samples) and 37°C (TSC3 complexes). Viscosities ranged between 0.8898–1.1441 cP (25°C) and 0.6895–0.9232 cP (37°C) and refractive indices (RI) were between 1.3301 and 1.3416.

Morphology Analysis

The morphology of TSC3/HPβ-CD was analyzed by Atomic Force Microscopy (AFM, Nanoscope IIIa Multimode-AFM, Quadrex, Digital Instruments, Veeco

Metrology, USA) employing the tapping mode. Prior to the analysis, the complex aqueous dispersion was diluted (50-fold, from 15.0% to 0.3% w/v final concentration). The diluted sample (2 μL, 4.67 μM/2.94 mM TSC3 and CD concentrations, respectively) was deposited onto a freshly cleaved mica surface and blown dried with nitrogen. The AFM topography image was recorded in air, at room temperature, with a silicon MPP-11100 cantilever tip radius <10 nm, resonant frequency of 300 Khz, and spring constant of 40 N/m (NanoDevices, Digital Instruments, Veeco Metrology). Samples were visualized in a scanning area of 1 μm × 1 μm and flattened over a scan speed of 2 Hz to a small scale area of 97.5 nm × 97.5 nm using the WSxM 4.0 Beta 3.1 AFM software (Nanotec Elect SL, Centro Empresarial Euronova, Spain).

X-Ray Powder Diffraction Analysis (XRD)

To evaluate the crystallinity of pristine and complexed TSCs, XDR spectra of pure TSC3, native and modified CDs, freeze-dried TSC/CD inclusion complexes and PMs were obtained in an X-ray diffractometer (Philips X'Pert X-ray diffractometer, The Netherlands) equipped with a PW3710 unit, system of soller slits, and monochromator reception. An X-ray generator (Philips, type PW1830) with an X-ray tube Cu anode, working at 35 Kv voltages and 20 mA current was used. The diffractograms were taken between 2° < theta < 40° with a step angle of 0.02° in theta and count time of 2 s per step.

Thermal Analysis

The thermal properties were characterized by Differential Scanning Calorimetry (DSC, Mettler TA-400 Differential Scanning Calorimetry, USA). Samples (3–13 mg) of pristine TSC3, freeze-dried HPβ-CD, freeze-dried TSC3/HPβ-CD complex and PM were sealed in 40 μL Al-cruicible pans and heated from 25°C to 350°C at 10°C/min under nitrogen atmosphere. Thermal analyses were carried out in duplicate.

Proton Nuclear Magnetic Resonance Spectroscopy (^{1}H-NMR)

To gain further insight into the TSC/CD interaction in water, samples of pure TSC2, TSC3 and TSC4, freeze-dried CDs (Mβ-CD, HPβ-CD and γ-CD) and TSC/CD inclusion complexes were analyzed by ^{1}H-NMR (500 MHz Bruker® Avance II High Resolution spectrometer, Bruker BioSpin GmbH, Germany), at 298°K. Pristine TSCs were analyzed in deuterium oxide (D_2O):DMSO-d_6 (34:66) solutions due to their extremely low intrinsic aqueous solubility. Other samples were analyzed in D_2O. To improve the chances of TSC detection, highly concentrated TSC/CD systems (30 mM, 500 μL) were used. NMR spectra were obtained with Bruker TOPSPIN 2.1 software (Bruker BioSpin GmbH, Germany). ^{1}H-NMR chemical shifts of Mβ-CD, HPβ-CD and γ-CD before and after the complexation of the corresponding TSC were expressed as Δδ (ppm) according to Eq. 4 (37):

$$\Delta\delta = \delta_{\text{TSC/CD complex}} - \delta_{\text{free-CD}} \quad (4)$$

Positive and negative signs indicated downfield and upfield shifts, respectively.

Physical Stability of TSC/CD Inclusion Complexes

To evaluate the physical stability of TSC3 systems, complexes in water were stored at 25°C and 37°C and the TSC concentration monitored over 1 week by UV spectrophotometry (see above). All the assays were conducted in triplicate and results are expressed as the mean concentration of TSC3 remaining in solution ± S.D. An additional physical instabilization phenomenon stems from the gradual self-aggregation of TSC/CD complexes. This aggregation not always results in TSC concentration loss. In this context, the size and PDI of TSC3/CD systems were followed up by DLS. Results are expressed as the mean of at least four measurements ± S.D.

Data Analysis

Values are represented as the mean ± S.D. The statistical analysis was performed by a one-way ANOVA (5% significance level, P values greater than 0.05 were considered statistically significant) combined with the Dunnett Multiple Comparison Test or t-test (5% significance level, P values greater than 0.05 were considered statistically significant). The software used was GraphPad Prism version 5.00 for Windows (GraphPad Software Inc., USA).

RESULTS

Phase-Solubility Studies

The stoichiometry of TSC/CD inclusion complexes was obtained from phase-solubility plots (38). Phase-solubility diagrams of TSC/CD inclusion complexes indicated the formation of Type A systems; the gradual increase of the CD concentration results in the increase of the TSC aqueous solubility. These plots usually show a turning point above certain CD concentration, where the drug concentration remains constant, irrespectively of the increase of the CD concentration (38). In general, TSC/CD complexes of TSC2 and TSC3 displayed linear relationships without a solubilization plateau for the evaluated CD

concentration range; these plots were indicative of A_L pattern. In these cases, the CD concentration employed was limited by (i) the maximum aqueous solubility of the specific CD or by (ii) the viscosity of the CD water solution (30) (Fig. S1). TSC4/γ-CD followed a similar linear trend (Fig. S1l). Conversely, TSC1/HPβ-CD, TSC1/Mβ-CD and TSC3/α-CD showed a negative deviation from linearity, indicating a A_N pattern (Table I; Figs. S1a,e,n) (22,37). Complexes of TSC4 with HPβ-CD and Mβ-CD presented a type A_p curve (Figs. S1d,h). These results were indicative of a 1:1 stoichiometry complex in the initial linear portion of the plot (when lower CD concentrations were used) and a 1:2 one at higher concentrations (above 45% for HPβ-CD and 15% for Mβ-CD). In these cases, $k_{1:1}$ and CE values of TSC4/Mβ-CD and TSC4/HPβ-CD were estimated from the initial linear portion of the solubility plots using Eq. 2 (24). The calculation of $k_{1:2}$ values was beyond the scope of this work.

To compare the solubilization capacity among CDs and the maximum solubilization capacity of each system, two parameters ($F_{3\%}$ and F_{max}) were calculated (Table I). Results indicated that Mβ-CD displays the greatest solubilization capacity followed by HPβ-CD. This behavior was consistent for all the TSCs. For example, $F_{3\%}$ and F_{max} values of TSC3 in 60% Mβ-CD were 14.6 and 203.9, respectively (Table I); the aqueous solubility increasing from 1.5 to 305.9 μg/mL. It is noteworthy that these CDs show the greatest intrinsic water solubility (up to 60%). Conversely, γ-CD showed a less effective complexation capacity and formed relatively weak complexes. For example, $k_{1:1}$ of TSC1/γ-CD and TSC2/γ-CD were 55.4 and 94.7 M^{-1}, respectively. It is noticeable that γ-CD water solubility is approximately 22%. Having expressed this, when identical concentrations were compared in A_L type systems, modified β-CDs always showed the best complexation performance of all the CDs (see $F_{3\%}$, Table I). The remaining TSC/CD inclusion complexes showed $k_{1:1}$ values within the expected range, indicating appropiate complexation. Interestingly, while the highest slope (0.0239) and CE (24.487×10^{-3}) corresponded to TSC1/Mβ-CD, followed by TSC1/HPβ-CD (0.0127 and 12.866×10^{-3}, respectively), these complexes did not display the highest $k_{1:1}$ values and the greatest increase in solubility (expressed as F_{max}, Table I). The highest constant values were obtained for TSC3/α-CD (514.2 M^{-1}), TSC2/Mβ-CD (435.8 M^{-1}) and TSC3/Mβ-CD (425.0 M^{-1}); these values were accompanied by relatively high $F_{3\%}$ and F_{max} (except for the F_{max} value of TSC3/α-CD; Table I). It is noticeable that α-CD water solubility is limited to approximately 14%. Conversely, TSC4/Mβ-CD showed the highest F_{max} of all the TSCs/CDs (215.3), while $k_{1:1}$ and CE values remained relatively low.

Determination of Residual Organic Solvents

The presence of organic solvent residues could lead to cytotoxic effects during the *in vitro* biological evaluation of the TSCs in cell monolayers. To ensure the complete elimination of the solvents employed during the preparation of the complexes, samples were analyzed by GC. The concentration of residual MeOH was smaller than 100 ppm. The maximum concentration allowed by the European Pharmacopeia is 3000 ppm (39).

Table I Apparent Stability Constants ($k_{1:1}$), Complexation Efficiency (CE), and Solubility Factors ($F_{3\%}$ and F_{Max}) of TSC/CD Complexes

TSC	Cyclodextrin	Slope	R^2	CE (10^{-3})	$K_{1:1}$ (M^{-1})[a]	Solubility type diagram	$F_{3\%}$ (±S.D.)	F_{max} (±S.D.)
TSC1	HPβ-CD	0.0127	0.9971	12.866	202.9	A_N[b]	3.7 (0.1)	21.6 (2.6)
	Mβ-CD	0.0239	0.9941	24.487	386.2	A_N[b]	11.2 (0.7)	96.4 (3.5)
	γ-CD	0.0035	0.9896	3.513	55.4	A_L	3.0 (1.5)	10.9 (1.6)
TSC2	HPβ-CD	0.0032	0.9892	3.211	253.0	A_L	9.7 (0.9)	107.1 (20.0)
	Mβ-CD	0.0055	0.9937	5.530	435.8	A_L	21.7 (4.0)	207.4 (4.3)
	γ-CD	0.0012	0.9354	1.202	94.7	A_L	9.0 (3.6)	24.3 (8.8)
TSC3	α-CD	0.0029	0.9998	2.910	514.2	A_N[b]	11.5 (8.1)	35.8 (9.8)
	HPβ-CD	0.0007	0.9848	0.701	123.8	A_L	10.1 (3.3)	64.8 (0.2)
	Mβ-CD	0.0024	0.9984	2.406	425.0	A_L	14.6 (2.4)	203.9 (12.5)
	γ-CD	0.0011	0.9944	1.101	194.6	A_L	4.4 (2.0)	41.5 (8.7)
	HPγ-CD	0.0010	0.9775	1.001	176.9	A_L	13.7 (2.2)	41.8 (7.5)
TSC4	HPβ-CD	0.0014	0.9934	1.402	186.2	A_p[b]	7.1 (1.3)	122.2 (20.8)
	Mβ-CD	0.0010	0.9899	1.001	133.0	A_p[b]	3.7 (0.9)	215.3 (18.2)
	γ-CD	0.0011	0.9713	1.101	146.3	A_L	4.8 (1.2)	26.1 (2.7)

[a] Intrinsic aqueous solubility values: TSC1 = 6.341 10^{-5} M; TSC2 = 1.269 10^{-5} M; TSC3 = 5.660 10^{-6} M; TSC4 = 7.528 10^{-6} M (Taken from Ref. 21)

[b] $k_{1:1}$ was estimated from the initial linear portion of the solubility plot (Taken from Ref. 22 and 37).

TSC/CD Interaction

Aiming to confirm the formation of inclusion complexes and gain insight into the TSC/CD interactions, samples of different complexes were studied by ATR/FT-IR spectroscopy and compared to pure TSCs and PMs (41,42). The characteristic bands of –NH streching of the terminal $–NH_2$ group for TSC1, TSC2 and TSC3 were found at 3375.4–3371.4 and 3263.3–3259.3 cm^{-1}, and the band of –*NH*-C(S)-NH_2 streching at 3153.4–3149.4 cm^{-1}, respectively. In the case of TSC4, the characteristic bands of -NH streching were found at 3354.9 and 3205.9 cm^{-1} (21). On the other hand, characteristic band of C = N stretching in the different TSCs was observed at 1604.3–1594.5 cm^{-1} (Fig. S2). In all the PMs, these signals were still apparent, while in TSC/CD complexes, these bands disappeared completely.

Self-Aggregation Behavior of Drug-Free CDs

The aggregation of drug-free CDs was primarily assessed (30,32,33). Intensity data (in derived count rates) was plotted for growing CD concentrations (Fig. S3). A sharp increase in the scattering intensity was observed upon aggregation. The intersection between the two straight lines corresponded to the *CAC* (33). β-CD showed the smallest value (1.87 mM), consistent with its low aqueous solubility (Table II). Native α-CD and γ-CD *CACs* were slightly more soluble, *CAC* values being 6.43 and 12.00 mM, respectively. Then, the chemical modification of β-CD led to remarkably greater *CAC* of 21.43 and 85.00 mM, for HPβ-CD and Mβ-CD, respectively.

The size and size distribution of the different CDs were also characterized. Unmodified CDs displayed unimodal size distributions with D_h at the *CAC* between 172.0 and 230.7 nm (Table II); the smaller the *CAC* (and the lower the solubility of the CD), the smaller the size of the aggregates. CD "monomeric" units (1–2 nm) were not observed. More water-soluble CDs presented a bimodal size pattern: (i) a major population (84.8%–88.8%) of aggregates with D_h of 180.9, 282.6 and 158.1 nm for HPβ-CD, Mβ-CD and HPγ-CD, respectively (Table II, peak 1) and (ii) a small population (11.2%–15.2%) of non-aggregated CD molecules (D_h = 1.4–1.7 nm) (Table II, peak 2).

Self-Aggregation Behavior of TSC/CD Inclusion Complexes

The different TSC/CD inclusion complexes were thoroughly characterized by DLS. TSC/unmodified CDs showed D_h between 199 and 830 nm and monomodal aggregation patterns (Table III). This phenomenon was irrespective of the CD type. In addition, the greater the CD concentration in the system, the larger the size of the structure observed (Table III) (30). It is important to note that TSC/γ-CD and TSC/α-CD complexes were opalescent, even at day 0. The size and size distribution as well as a scheme of the possible aggregation pattern are exemplified for TSC3/Mβ-CD in Fig. 2. TSC/HPβ-CD complexes containing 60% CD were not measurable by DLS due to a high viscosity (1.4718 cP at 25°C) and a strong aggregation tendency that resulted in PDI values >0.8.

Z-potential is a useful tool to characterize the surface charge density of the CDs (43,44). TSC-free CD and TSC/CD displayed negative values. TSC3/HPβ-CD complexes ranged between −41.90 mV (0.5% w/v) and −2.44 mV (60.0% w/v), at day 0 and remained constant over 1 week (Fig. 3). This behavior was consistent for all the concentration range, except for 0.5% and 1.5% that, at day 7, decreased from −41.90 to −25.2 mV. The smaller the size of the TSC3/HPβ-CD complex measured by DLS (Table III), the more negative the Z-potential value (Fig. 3). For example, a size of 152.4 nm corresponded to a Z-potential of −41.90 mV (TSC3/HPβ-CD 0.5%), while a size of

Table II Critical Aggregate Concentration (*CAC*) in milli-Q water at 25°C and Hydrodynamic Diameter (D_h) of Native and Modified Drug-Free CD Aggregates Measured by DLS

Cyclodextrin	*CAC*		Mean size of CD-aggegates and monomeric forms at *CAC*				
	mM	% (w/v)	Peak 1		Peak 2		PDI (±S.D.)
			Dh (nm) (±S.D.)	% (±S.D.)	*Dh* (nm) (±S.D.)	% (±S.D.)	
α-CD	6.43	0.63	188.6 (11.7)	100.0 (0.0)	–	–	0.627 (0.185)
β-CD	1.87	0.21	172.0 (43.9)	100.0 (0.0)	–	–	0.200 (0.118)
γ-CD	12.00	1.55	230.7 (20.3)	100.0 (0.0)	–	–	0.103 (0.076)
HPβ-CD	21.43	3.00	180.9 (4.5)	88.8 (1.6)	1.4 (0.3)[a]	11.2 (1.6)	0.457 (0.041)
Mβ-CD	85.00	11.00	282.6 (27.0)	84.8 (1.1)	1.6 (0.0)[a]	15.2 (1.1)	0.678 (0.102)
HPγ-CD	57.20	9.00	158.1 (16.7)	87.6 (1.9)	1.7 (0.1)[a]	12.4 (1.9)	0.339 (0.038)

[a] Monomeric forms of chemically-modified CDs.

Results are expressed as mean value of four measurements ± S.D.

Table III Hydrodynamic Diameter (D_h) of TSC/CD Complexes of Native and Modified CD, at day 0, as Measured by DLS

TSC	CD	CD Concentration (% w/v)	Peak 1		Peak 2		PDI (±S.D.)
			D_h (nm) (±S.D.)	% (±S.D.)	D_h (nm) (±S.D.)	% (±S.D.)	
TSC1	HPβ-CD	0.5	163.7 (2.7)	100.0 (0.0)	–	–	0.266 (0.009)
		1.5	154.4 (1.2)	100.0 (0.0)	–	–	0.181 (0.024)
		3.0	149.3 (1.5)	100.0 (0.0)	–	–	0.161 (0.013)
		15.0	255.8 (1.0)	100.0 (0.0)	–	–	0.127 (0.025)
		30.0	390.5 (3.8)	100.0 (0.0)	–	–	0.119 (0.093)
	Mβ-CD	0.5	195.2 (3.3)	100.0 (0.0)	–	–	0.058 (0.011)
		1.5	268.9 (9.9)	100.0 (0.0)	–	–	0.086 (0.029)
		3.0	220.3 (5.7)	100.0 (0.0)	–	–	0.088 (0.045)
		15.0	420.5 (54.6)	91.5 (1.0)	2.0 (0.1)	8.5 (1.0)	0.363 (0.065)
		30.0	494.6 (89.3)	89.2 (0.4)	2.5 (0.1)	10.8 (0.4)	0.532 (0.091)
	γ-CD	0.5	199.6 (21.1)	100.0 (0.0)	–	–	0.234 (0.091)
		1.5	272.2 (14.6)	100.0 (0.0)	–	–	0.297 (0.082)
		3.0	769.7 (139.6)	100.0 (0.0)	–	–	0.198 (0.042)
		7.5	296.8 (8.2)	100.0 (0.0)	–	–	0.128 (0.026)
		15.0	648.7 (22.3)	100.0 (0.0)	–	–	0.074 (0.030)
		22.0	830.0 (10.9)	100.0 (0.0)	–	–	0.089 (0.064)
TSC2	HPβ-CD	0.5	152.5 (12.9)	93.5 (0.3)	1.8 (0.1)	6.5 (0.3)	0.296 (0.023)
		1.5	121.2 (5.4)	91.4 (0.7)	1.8 (0.1)	8.6 (0.7)	0.398 (0.053)
		3.0	126.0 (2.4)	100.0 (0.0)	–	–	0.088 (0.014)
		15.0	215.2 (5.2)	100.0 (0.0)	–	–	0.119 (0.018)
		30.0	357.3 (3.2)	100.0 (0.0)	–	–	0.248 (0.007)
	Mβ-CD	0.5	203.9 (2.2)	100.0 (0.0)	–	–	0.316 (0.033)
		1.5	183.9 (2.3)	100.0 (0.0)	–	–	0.055 (0.024)
		3.0	181.9 (6.4)	100.0 (0.0)	–	–	0.091 (0.038)
		15.0	332.7 (11.2)	92.5 (0.1)	2.1 (0.1)	7.5 (0.1)	0.389 (0.079)
		30.0	483.2 (33.5)	85.7 (0.5)	2.3 (0.1)	14.3 (0.5)	0.567 (0.051)
	γ-CD	0.5	248.0 (9.5)	100.0 (0.0)	–	–	0.182 (0.028)
		1.5	234.1 (3.2)	100.0 (0.0)	–	–	0.236 (0.020)
		3.0	268.6 (5.1)	100.0 (0.0)	–	–	0.204 (0.005)
		7.5	261.2 (13.7)	100.0 (0.0)	–	–	0.227 (0.013)
		15.0	502.3 (23.1)	100.0 (0.0)	–	–	0.224 (0.018)
		22.0	215.6 (11.3)	100.0 (0.0)	–	–	0.744 (0.016)
TSC3	α-CD	0.5	309.6 (13.1)	100.0 (0.0)	–	–	0.368 (0.082)
		1.5	395.4 (23.0)	100.0 (0.0)	–	–	0.344 (0.040)
		3.0	471.4 (31.9)	100.0 (0.0)	–	–	0.264 (0.015)
		7.5	473.0 (29.6)	100.0 (0.0)	–	–	0.312 (0.032)
		10.0	897.6 (180.1)	100.0 (0.0)	–	–	0.205 (0.013)
		14.0	736.4 (12.7)	100.0 (0.0)	–	–	0.175 (0.044)
	HPβ-CD	0.5	152.4 (19.1)	90.8 (1.1)	1.4 (0.4)	9.2 (1.1)	0.380 (0.013)
		1.5	153.5 (1.5)	100.0 (0.0)	–	–	0.171 (0.006)
		3.0	176.9 (13.7)	57.9 (4.2)	2.0 (0.0)	42.1 (4.2)	0.333 (0.116)
		15.0	191.9 (7.5)	59.7 (0.1)	2.0 (0.0)	40.3 (0.1)	0.871 (0.012)
		30.0	250.8 (26.3)	52.3 (4.3)	2.3 (0.1)	47.7 (4.3)	0.354 (0.031)
	Mβ-CD	0.5	212.3 (7.9)	100.0 (0.0)	–	–	0.027 (0.031)
		1.5	289.4 (12.9)	100.0 (0.0)	–	–	0.122 (0.038)
		3.0	270.4 (10.3)	100.0 (0.0)	–	–	0.192 (0.026)
		15.0	250.1 (57.2)	67.3 (3.0)	1.9 (0.0)	32.7 (3.0)	0.420 (0.011)

Table III (continued)

TSC	CD	CD Concentration (% w/v)	Peak 1		Peak 2		PDI (±S.D.)
			D_h (nm) (±S.D.)	% (±S.D.)	D_h (nm) (±S.D.)	% (±S.D.)	
		30.0	606.7 (140.7)	58.2 (2.9)	2.4 (0.1)	41.8 (2.9)	0.813 (0.022)
	γ-CD	0.5	256.3 (20.6)	100.0 (0.0)	–	–	0.193 (0.147)
		1.5	305.7 (49.8)	100.0 (0.0)	–	–	0.227 (0.004)
		3.0	256.0 (10.8)	100.0 (0.0)	–	–	0.137 (0.024)
		7.5	421.2 (23.1)	100.0 (0.0)	–	–	0.226 (0.014)
		15.0	368.9 (44.4)	100.0 (0.0)	–	–	0.267 (0.017)
		22.0	676.1 (60.9)	100.0 (0.0)	–	–	0.088 (0.062)
	HPγ-CD	0.5	246.6 (11.9)	100.0 (0.0)	–	–	0.346 (0.029)
		1.5	147.2 (10.5)	100.0 (0.0)	–	–	0.295 (0.045)
		3.0	191.5 (12.9)	100.0 (0.0)	–	–	0.176 (0.043)
		7.5	219.6 (15.9)	100.0 (0.0)	–	–	0.260 (0.014)
		15.0	313.7 (13.3)	100.0 (0.0)	–	–	0.206 (0.012)
		30.0	505.5 (47.6)	100.0 (0.0)	–	–	0.435 (0.072)
TSC4	HPβ-CD	0.5	178.1 (37.6)	100.0 (0.0)	–	–	0.232 (0.071)
		1.5	197.5 (2.6)	100.0 (0.0)	–	–	0.080 (0.026)
		3.0	194.6 (8.1)	100.0 (0.0)	–	–	0.087 (0.033)
		15.0	688.7 (30.3)	100.0 (0.0)	–	–	0.158 (0.031)
		30.0	2213.3 (265.9)	70.9 (3.8)	291.9 (23.1)	29.1 (3.8)	0.542 (0.057)
	Mβ-CD	0.5	150.9 (5.2)	100.0 (0.0)	–	–	0.044 (0.032)
		1.5	197.7 (5.7)	100.0 (0.0)	–	–	0.074 (0.015)
		3.0	194.7 (6.4)	100.0 (0.0)	–	–	0.063 (0.021)
		15.0	468.7 (78.9)	88.6 (0.9)	1.7 (0.1)	11.4 (0.9)	0.410 (0.035)
		30.0	2153.4 (80.6)	78.1 (3.0)	1.3 (0.2)	21.9 (3.0)	0.962 (0.021)
	γ-CD	0.5	204.6 (3.4)	100.0 (0.0)	–	–	0.122 (0.024)
		1.5	448.0 (15.1)	100.0 (0.0)	–	–	0.313 (0.111)
		3.0	269.9 (24.4)	100.0 (0.0)	–	–	0.227 (0.046)
		7.5	419.0 (44.6)	100.0 (0.0)	–	–	0.321 (0.106)
		15.0	347.4 (11.1)	100.0 (0.0)	–	–	0.242 (0.145)
		22.0	627.3 (0.6)	100.0 (0.0)	–	–	0.086 (0.083)

Results are expressed as the mean value of four measurements ± S.D.

250.8 nm to −5.23 mV (TSC3/HPβ-CD 30.0%). Pristine drug-free CDs followed a similar trend with values of −20.03 and −2.17 mV for 0.5% and 60.0% systems, respectively.

Preliminary biological data *in vitro* suggested that TSC3 displays the greatest antiviral activity against BVDV of all the derivatives (17). Thus, TSC3 was chosen to further evaluate the activity against HBV and HCV in cellular constructs. In advance, the work was focused on the more extensive characterization of TSC3 complexes to choose the complex that displays more advantageous features towards these studies.

Morphology Analysis

The morphology of TSC3/HPβ-CD was studied by AFM. CD systems need to be appropriately diluted before analysis (45). To comply with this condition, a sample originally containing 15% CD was diluted 1:50, resulting in a 0.3% CD final concentration. TSC3/HPβ-CD presented relatively small structures with a diameter of approximately 20 nm and a height of 50 nm (Fig. 4). SEM and TEM (data not shown) did not contribute to gain additional insight into the structure of the complexes.

Crystallinity Analysis

To study the nature of TSC3 (crystalline or amorphous) in the corresponding complex, samples with Mβ-CD, HPβ-CD and γ-CD were analyzed by XRD and DSC. These two techniques are gold standards for the analysis of CD complexes. Pure TSC3 showed the pattern of a characteristic crystalline powder. TSC3/CD complex powders

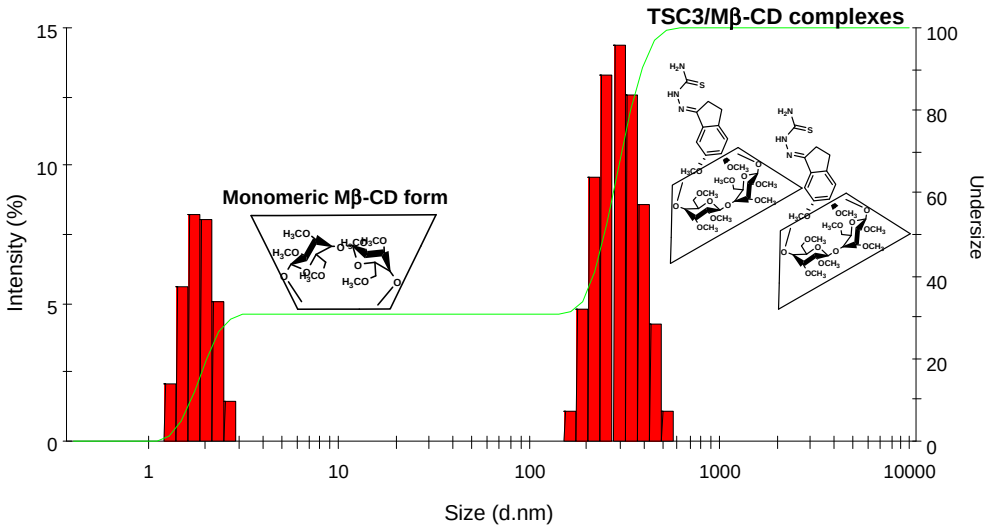

Fig. 2 Representative mean size and size distribution by intensity TSC3/Mβ-CD (15% w/v) inclusion complexes in water, at day 0. The populations displaying D_h of 1.9 (30.5%) and 302.4 nm (69.5%) would correspond to CD monomers and TSC/CD aggregates, respectively; monomers were detected even after 1 week.

appeared as completely amorphous (Fig. 5a,b). On the other hand, these signals were also lost in PMs, owing to the extremely low TSC relative concentration; the PM contained a TSC/CD weight ratio identical to that of the complex (Fig. 5b). Similarly, TSC was not detectable in the PM and in the complex by DSC (not shown).

TSC/CD Interaction in Solution

Liquids ^{1}H-NMR is one of the ultimate techniques to investigate the drug/CD interaction in liquid state. Since the TSC water solubility is extremely low as well as the sensitivity of ^{1}H-NMR, pure TSC3 was analyzed in D_2O: DMSO-d_6 (34:66). Lyophilized TSC/CD inclusion complexes and TSC-free CDs were analyzed in 100% D_2O. Since the protons of TSC were not apparent, the analysis was focused on the thorough evaluation of the chemical shifts undergone by the signals of specific CD protons; the assumption is that these shifts are caused by the interaction of the CD with the TSC. HPβ-CD and γ-CD signals shifted downfield, irrespectively of the TSC. Upfield shifts were observed for the complexes of TSC2 and TSC4 with Mβ-CD. For example, TSC4/CD showed the upfield shift of CD-H5 and the disappearance of CD-H6, when compared to the other complexes. The ^{1}H-NMR chemical shifts, as calculated with Eq. 3, are summarized in Table SI.

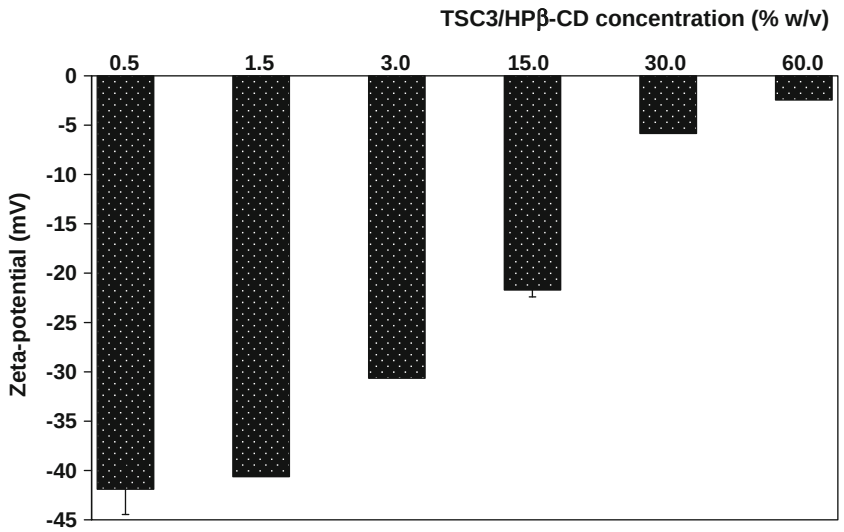

Fig. 3 Representative Z-potential values of the TSC3/HPβ-CD complex as a function of HPβ-CD concentrations.

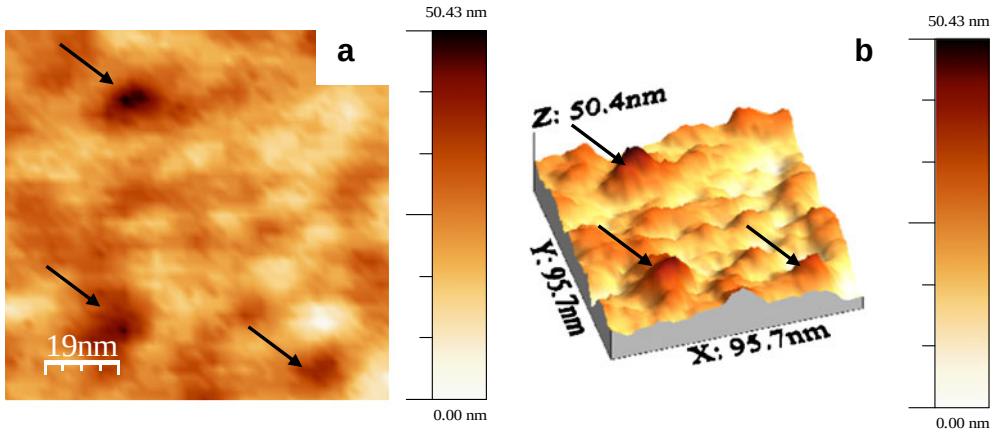

Fig. 4 Representative Tapping-Mode Atomic Force Microscopy (TM-AFM) topographic flatten zoom image of a thin film of TSC3/HPβ-CD inclusion complex at 0.3% w/v CD final concentration. (**a**) *2D* TM-AFM image, scale bar: 19 nm and (**b**) *3D* TM-AFM image. Scan range: 95.7 nm.

Physical Stability of the Complexes

The stability of TSC3/CD complexes was evaluated over 1 week by means of TSC3 concentration and DLS, at 25 and 37°C. Regardless of the CD employed and the concentration, TSC3/α-CD and TSC3/γ-CD were highly stable in the whole concentration range, at 25°C (Fig. 6a,d). In contrast, TSC3/HPβ-CD, TSC3/HPγ-CD and TSC3/Mβ-CD showed good stability only until day 1 (Fig. 6b,c,e). TSC/Mβ-CD complexes showed the greatest increase in solubility of all TSCs but were the less stable systems over time; this behavior was more pronounced for high CD concentrations.

D_h data indicated that the greater the CD concentration, the larger the size of the aggregates at day 0. These findings were consistent with the self-aggregation of CDs. Most of the complexes were quite stable at day 1. However, aggregation was not totally curtailed (Fig. 7). α-CD and γ-CD complexes were highly stable in terms of TSC solubility (Fig. 6a,d), though sizes (DLS) were remarkably large from day 0 (Table III, Fig. 7a,d); these CDs display the smallest *CAC* and the greatest self-aggregation tendency of all the series. In addition, opalescence will probably preclude the biological evaluation of these systems in cell cultures. In contrast, complexes of chemically-modified CDs showed a steady size growth usually between days 1 and 7. This phenomenon was especially fast for TSC3/Mβ-CD, TSC4/Mβ-CD and TSC4/HPβ-CD (30% w/v), that showed sizes greater than 2 μm (and PDI>0.8), even at day 0. Conversely, the size of TSC3/HPβ-CD and TSC3/HPγ-CD increased significantly but they did not grow above 348–600 nm. It is remarkable that these systems remained macroscopically translucent.

When the stability of TSC3/HP-βCD was assessed at 37°C, initial sizes and physical stability profiles were similar to those observed at 25°C (Table SII). Further stability studies in culture medium with and without serum will be conducted in parallel to the biological activity assays.

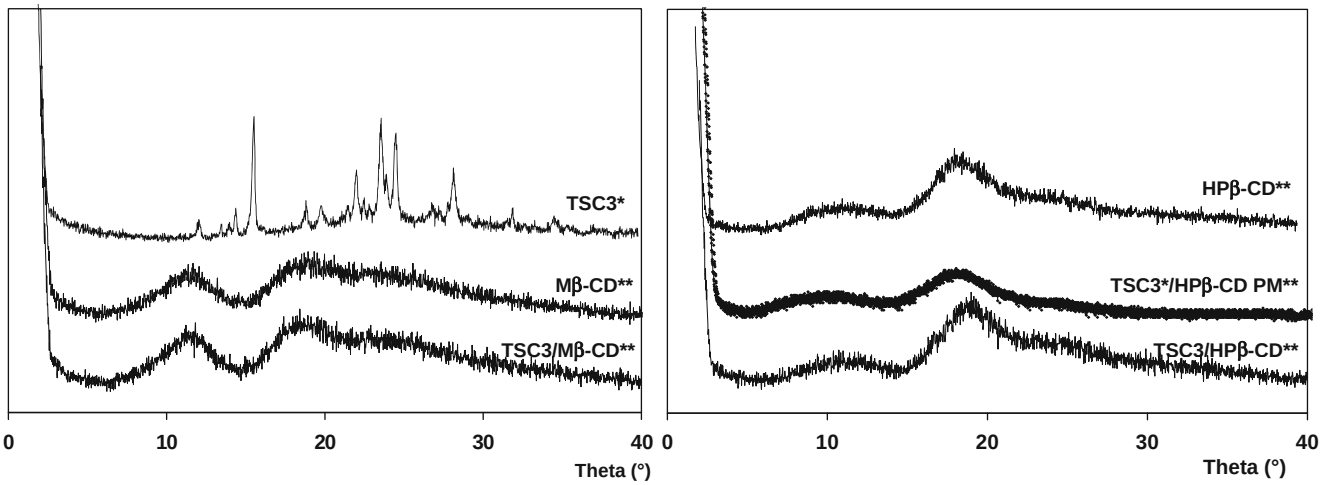

Fig. 5 X-ray diffractograms of pristine TSC3 (*) and freeze-dried samples (**).

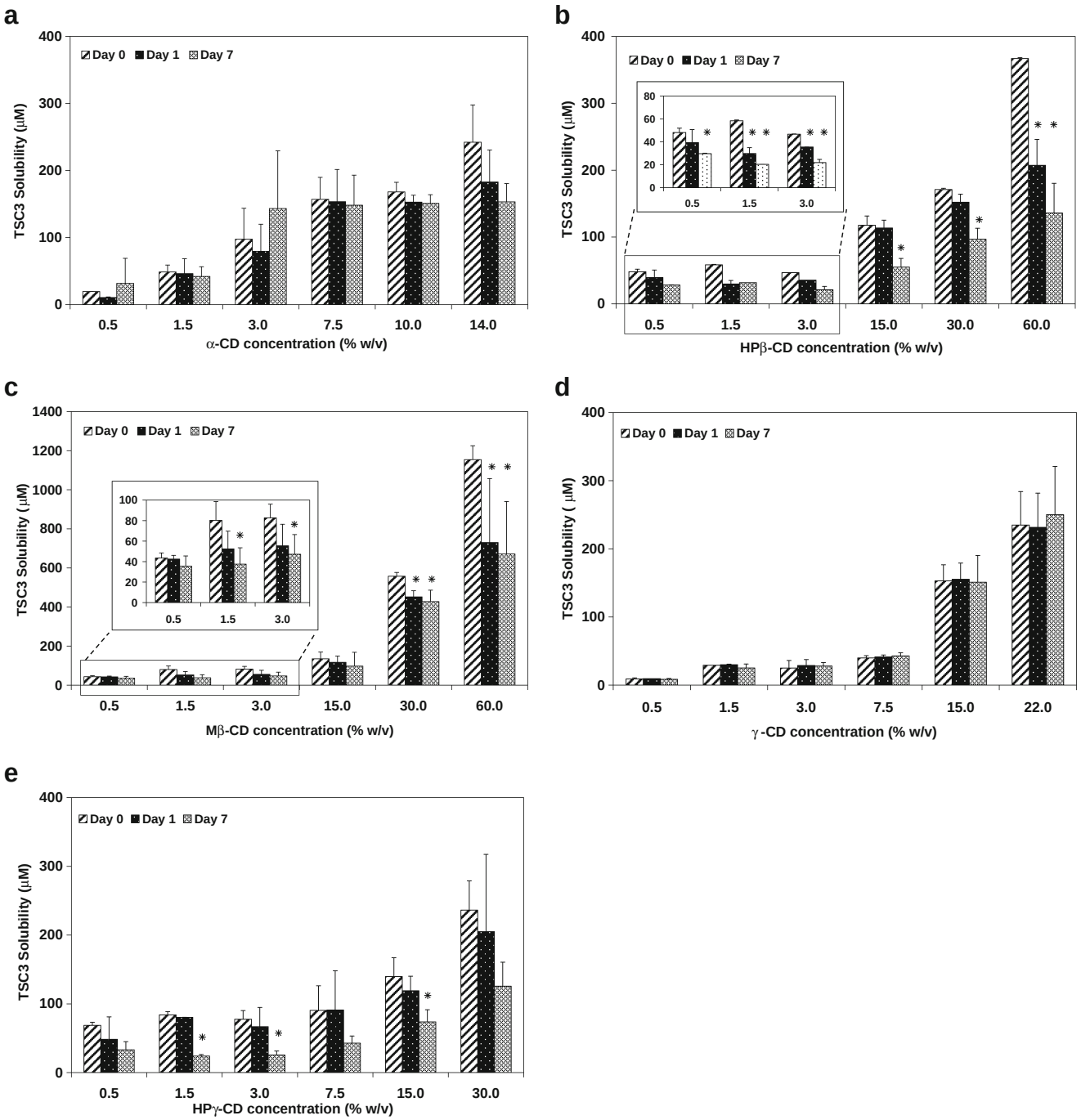

Fig. 6 Physical stability of TSC3/CD inclusion complex solutions as estimated by TSC concentration at 25°C, over 1 week. (**a**) TSC3/α-CD, (**b**) TSC3/HPβ-CD, (**c**) TSC3/Mβ-CD, (**d**) TSC3/γ-CD and (**e**) TSC3/HPγ-CD. Results are expressed as mean value of three samples ± standard deviation (SD). *Statistically significant decrease of TSC concentration when compared to the TSC concentration in the complex at day 0 ($P < 0.05$).

DISCUSSION

To investigate the effect of the cavity size on the TSC complexation capacity, CDs displaying gradually larger cavities were investigated. In β-CD, a secondary belt is formed by the hydrogen bonds and this more rigid structure results in especially low water solubility (~1.85%) (24). Thus, the pristine β-CD was replaced by chemically modified derivatives (Mβ-CD and HPβ-CD) that display dramatically higher aqueous solubility, while maintaining the size of the hydrophobic cavity basically unchanged. These derivatives are known to be less cytotoxic and more verstatile to conduct a comprehensive complexation study due to the extremely high aqueous solubility (46).

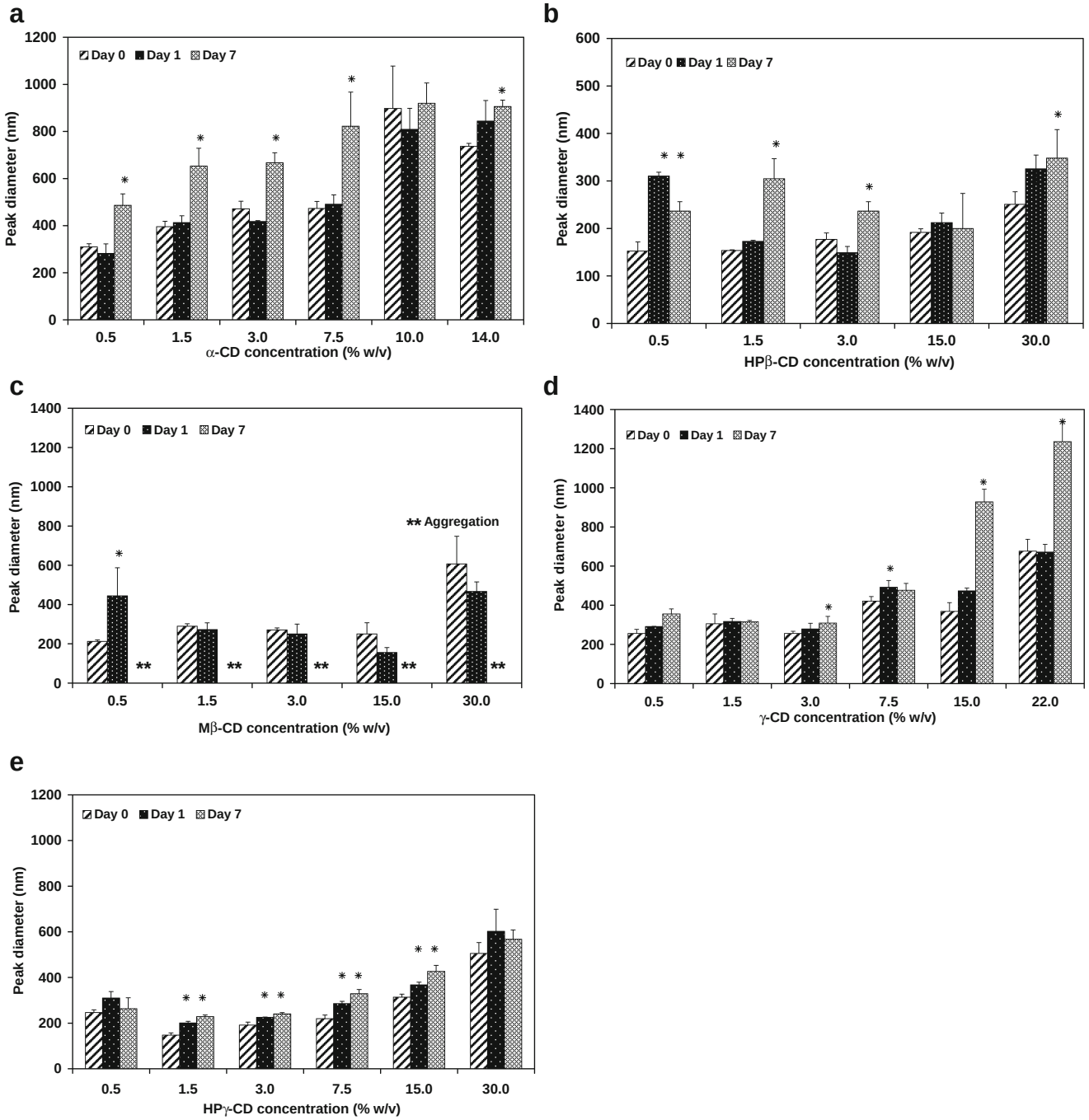

Fig. 7 Physical stability of TSC3/CD inclusion complexes in aqueous medium at 25°C as estimated by D_h, over 1 week. (**a**) TSC3/α-CD, (**b**) TSC3/HPβ-CD, (**c**) TSC3/Mβ-CD, (**d**) TSC3/γ-CD and (**e**) TSC3/HPγ-CD. Results are expressed as mean ± SD ($n = 4$). *Statistically significant increase of the TSC/CD complex Dh when compared to the TSC/CD complex Dh at day 0 ($P < 0.05$). **Aggregates samples were not measurable by DLS.

Drug/CD complexes in solution are dynamic systems where drug molecules interact with the CD surface and the CD cavity, forming inclusion complexes and non-inclusion (36) complexes that are characterized by an apparent stability constant ($k_{1:1}$) (34,35). Generally, ideal apparent stability constants ($k_{1:1}$) range between 50 to 2000 M^{-1} (22,30). Smaller experimental values indicate weak drug/CD interactions and are associated with a low CE, while greater values reveal extremely strong interactions that constrain the release of the drug from the CD cavity (40).

Most of the plots of N-unsubstituted TSCs were linear in the whole concentration range (A_L) or linear at low CD concentrations with a negative deviation from linearity at greater concentrations (A_N). These results indicated the

formation of complexes that comprise one CD molecule per TSC. Even though a slope smaller than the unity does not exclude the formation of higher order complexes, in the absence of additional data, a one-to-one complex is assumed (22). β-CD derivatives displayed the most effective complexation capacity, while γ-CD was the less effective CD. α-CD resulted in the solubilization of TSC3 to an intermediate extent. These findings would suggest that the size of the hydrophobic aromatic ring of indanone would fit the size of the β-CD cavity. α-CD probably bears a cavity that is too small to incorporate the TSC molecule and the cavity of γ-CD is too large. Thus, even if γ-CD incorporates TSC, it fails to generate sufficiently strong interactions and TSC molecules are released rapidly from the cavity to the aqueous medium (Table I). This hypothesis is strongly supported by the fact that complexes of TSC3 with γ-CD and HPγ-CD (two CDs with identical cavity diameter though different maximum aqueous solubility) displayed similar CE, $k_{1:1}$ and F_{max} values; this behavior was irrespective of the differential solubility profile. Moreover, the incorporation of CH_3O- functional groups to the aromatic ring and the enlargement of the hydrophobic portion of the molecule improved the TSC/γ-CD and TSC/HPβ-CD association and resulted in greater $k_{1:1}$ values (Table I). The remaining TSC/CD inclusion complexes showed $k_{1:1}$ within the expected range, indicating appropiate complexation. Interestingly, while the highest slope and CE values corresponded to TSC1/Mβ-CD and TSC1/HPβ-CD, these complexes did not display the highest $k_{1:1}$ and the greatest increase in solubility. This behavior relies on the fact that the solubility diagrams (A_N type curve) of these complexes displayed a negative deviation from linearity as a function of Mβ-CD and HPβ-CD concentration (approximately above 3% w/v). A_N profiles may be associated with both the self-association of drug-free Mβ-CD (*CAC*=11%) and HPβ-CD (*CAC*=3%) at high concentrations and the modification in the effective nature of the solvent in the presence of a large amount of these CDs (22,37). The highest constant values were obtained for TSC3/α-CD (514.2 M^{-1}), TSC2/Mβ-CD (435.8 M^{-1}) and TSC3/Mβ-CD (425.0 M^{-1}); these values were accompanied by relatively high $F_{3\%}$ and F_{max} (except F_{max} value for TSC3/α-CD). The reason for this exception was that TSC3/α-CD displayed an A_N plot with the negative deviation from linearity at concentrations above 1.5%. At higher concentrations, α-CD showed a greater aggregation tendency (*CAC*=0.63%) that affect negatively the TSC3 solubilization efficiency. On the other hand, it is worth stressing that even though the complexes formed are 1:1 type, TSC and CD are not in equimolar ratio. This behavior is evidenced by the relatively large molar amount of CD required to complex much smaller molar amounts of TSC, and indicates the presence of free CD molecules. In other words, a large CD molar excess is required to "force" free TSCs to interact with free CD molecules in the medium (9,26,36).

TSC4/HPβ-CD and TSC4/Mβ-CD at CD concentrations greater than 45 and 15% w/v, respectively, showed a positive curvature that indicated the formation of A_p complexes containing two CD molecules per TSC4 (22,24). The fact that these complexes are formed only at high concentrations of chemically-modified and with the only N-substituted TSC suggested that the N-allyl group plays a key role. A mechanism that *a priori* could explain the appearance of 1:2 complexes is the partial formation of non-inclusion complexes through the interaction of TSC molecules with the CD surface (24). Data of N-unsubstituted TSC complexes suggested that they do not form this type of complex, in the whole concentration range. Since N-substituted TSCs are more hydrophobic molecules, they would be even less prone to interact with the hydrophilic surface of pristine CDs. In fact, TSC4 complexes with γ-CD showed a 1:1 pattern over the whole concentration range. A similar trend was observed with HPβ-CD and Mβ-CD, two CDs that display identical cavity and different superficial hydrophilicity, at low CD concentrations. Thus, the change in the complexation pattern of TSC4 at greater CD concentrations would rely on the interaction of the allyl group of TSC4 with the surface of the less hydrophilic chemically-modified CDs; the interaction with more hydrophobic $-CH_3$ of Mβ-CD being stronger than that with the more hydrophilic –OH of HPβ-CD and taking place at a lower CD concentration. This hypothesis is supported by the sharp size increase showed by these systems in DLS (D_h>2 μm).

It is noteworthy that $k_{1:1}$ is not the ultimate parameter to establish the role played by the cavity size in the complexation and a thorough analysis of the whole data needs to be addressed.

The formation of TSC/CD inclusion complexes was unequivocally confirmed in dry samples analyzed by ATR/FT-IR, where the characteristic TSC band disappeared completely as opposed to PMs. Further evidence of the nature of the complexes was gained by liquid ^{1}H-NMR; the complexation is revealed by the shifting and/or disappearance of drug and/or CD proton signals when the inclusion complex is formed (37,47). The minimum concentration of TSC that could be previously detected in the NMR apparatus was 250 μM, but 2500 μM had a better sensibility (21). According to phase solubility diagrams (Fig. S1), the predicted TSC amount concentration in the complex should have been sufficiently high to be detected by ^{1}H-NMR. However, TSC protons were not observed in NMR spectra of the inclusion complexes. These findings were in full agreement with FT-IR data.

The incorporation of TSC into the CD cavity was further evaluated by calculating the shift of CD protons. CD-H3 and CD-H5 are located inside the cavity, CD-H6 at the narrow-rim and CD-H1 on the surface of the CD molecule. In general, when there is a guest/host interaction both down and upfield shifts can be expected (48–50). All the CD-Hs were affected to a greater or to a lesser extent. Generally, the greater the TSC hydrophobicity was, the stronger the shift. For example, in presence of TSC derivatives, HPβ-CD and γ-CD signals shifted downfield (Table SI). This phenomenon could be related to a deprotection or anisotropy effect due to the inclusion of the TSC hydrophobic aromatic ring into the CD cavity (37,48–50). In addition, CD-H1 downfield shift would stem from the TSC interaction with the CD surface, as suggested by Gibaud *et al.* (50). Even though data suggested that the formation of non-inclusion complexes is less feasible, the temporary interaction of TSCs with the CD surface in liquid state cannot be discarded. In addition, the upfield shift of CD-H5 in TSC4/CD could rely on the formation of an A_p-type 1:2 TSC/CD complex.

Ongoing molecular dynamic studies suggest that the TSC/CD interaction takes place through hydrogen bonding mainly inside the CD cavity and to a smaller extent with the CD surface (data not shown). These results would support the NMR results suggesting that, regardless of the molecular features, all the TSCs are completely incorporated into the CD cavity.

The self-aggregation of drug-free and drug-loaded CDs in water is a well-known phenomenon (28,30). The size and size distribution of the aggregates may affect the interaction with cells and affect the ability to cross biological barriers and the absorption process *in vivo*. First, the self-aggregation behavior of pure CDs was assessed. Despite the presence of functional groups on the surface that may hinder self-aggregation, both pristine and chemically modified CDs self-aggregated. The former showed unimodal size distributions, while the latter combined aggregates with a small fraction of non-aggregated CD. Interestingly, the contribution of the cavity size to the size of the aggregates appears to be negligible. A similar trend was followed by TSC/CDs complexes, this behavior being irrespective of the CD. Since the size of pure CD aggregates was 158–283 nm, data suggest that the TSC/CD self-aggregation is favored by the TSC that by itself self-aggregates (21). Also, the presence of a small fraction of monomeric CD (1.4–2.5 nm) in complexes of chemically modified CDs for concentrations greater than 3.0% indicated the coexistence of non-aggregated drug-free CDs and TSC/CD complexes and aggregated TSC/CD complexes (24).

Additional insight into the role played by the TSC in the self-aggregation process of TSC/CD complexes was gained by the analysis of the surface charge density. Even though values were always negative, the increase of the CD and TSC concentration in the system led to a sharp increase of the Z-potential to less negative values (Fig. 3). These results were in agreement with previous investigations (44) and would be associated with the self-aggregation of CDs and TSC/CD complexes, and translated into larger sizes by DLS (Table III). Moreover, this behavior further stresses the impact of the CD concentration on the aggregation pattern and their interaction with cells; due to presence of sialic acid residues in the cell membrane, cells display a negatively-charged surface. Moreover, less negative Z-potential values resulted in less physically stable systems, as electrostatic repulsion is a stabilization mechanism in colloids (see below).

The primary self-aggregation and later precipitation of TSC3 in aqueous media represents one of the main drawbacks towards the reliable evaluation of its antiviral activity. Since pure CDs and TSC3/CD complexes self-aggregate, the study of the physical stability of the different TSC3/CD systems in water was of special interest. *In vitro* antiviral experiments are usually conducted over 2–4 days and comprise the exchange of the culture medium (that contains the TSC/CD complex) every 24 h. Thus, to attain reliable results, TSC3/CD aqueous systems need to remain physically stable for at least 24 h; a new TSC/CD aqueous system is prepared every day. In general, the stability depended on (i) the CD type and (ii) CD (and TSC) concentration. The TSC3 concentration in α-CD and γ-CD remained almost unchanged (Fig. 6a,d). Complexes of chemically modified CDs were less stable and showed a gradual TSC concentration drop.

The relatively fast self-aggregation of pure 1-indanone TSCs in water:DMSO (98:2) has been previously reported (21). Remarkably, the formed nanoparticles remained invisible to the naked eye and no changes in the TSC concentration were measured. Thus, to complement the stability assays, the size of the TSC3/CD in water was also monitored over 1 week and compared to the initial size of the complex. Findings indicate that size growths take place faster and are more pronounced than the TSC concentration drop. This would probably stem from the initially fast self-aggregation of TSC3/CDs that favors, in a later stage, the nucleation and precipitation of free TSC3 molecules. Only then, a sharp decrease of TSC3 concentration is observed. In this regard, it should be stressed that the size growth of pure TSC particles will lead to the gradual decrease of the effective TSC concentration in the culture medium and the overestimation of the antiviral activity. In contrast, in the case of TSC/CD aggregates, the size growth will not necessarily mean that TSC will not be available to cells as complexes may serve as drug reservoirs that release the drug over time. Overall, CD complexation appears as a useful approach to physically stabilize TSC3 in aqueous medium for the period of the biological analysis.

TSC3/γ-CD probably showed the best equilibrium between complexation capacity and physical stability over time though the system was opalescent. Moreover, for identical CD concentrations, the HPβ-CD complex enables the attainment of greater absolute TSC concentrations. Since CDs display concentration-dependent cytotoxicity, TSC3/HPβ-CD would appear a more advantageous and versatile system to fine tuning the TSC/CD concentration balance. Moreover, TSC3/HPβ-CD aggregates are smaller; the smaller the size, the better the cellular uptake. Overall findings point out TSC3/HPβ-CD as the best candidate to pursue the TSC3 antiviral activity against HCV and HBV. However, this hypothesis will need to be confirmed in the *in vitro* assays.

CONCLUSIONS

The performance of different pristine and chemically modified CDs as drug carriers to improve the aqueous solubility and prevent the TSC self-aggregation in water has been exhaustively investigated. Significantly greater TSC concentrations with respect to the CD-free systems were attained. The order of TSC3 solubilization capacity was Mβ-CD >> HPβ-CD > γ-CD ~ HPγ-CD ~ α-CD. Even though complexation did not totally prevent self-aggregation, in general, TSC3/CD inclusion complexes in water were physically stable for at least 1 day, with no changes in TSC concentration and size. This improvement is very relevant for the ongoing biological experiments and will enable the reliable evaluation of the antiviral activity in different viral hepatitis cellular constructs.

ACKNOWLEDGMENTS & DISCLOSURES

R.J. Glisoni thanks the Ph.D. scholarship of CONICET. AS, AM and DC are staff members of CONICET. The authors thank Dr. Gloria Bonetto (Universidad Nacional de Córdoba, Córdoba, Argentina) for 1D-NMR analysis and Dr. Daniel R. Vega (Departamento Física de la Materia Condensada, CNEA, Buenos Aires, Argentina) for X-ray analysis.

REFERENCES

1. Atwood D, Florence AT. Surfactant Systems: Their Chemistry, Pharmacy and Biology. Chapter 3, Micellization, Chapman and Hall. 72–117 (1983).
2. Espada R, Valdespina S, Alfonso C, Rivas G, Ballesteros MP, Torrado JJ. Effect of aggregation state on the toxicity of different amphotericin B preparations. Int J Pharm. 2008;361:64–9.
3. Taboada P, Attwood D, Ruso JM, Sarmiento F, Mosquera V. Self-association of amphiphilic penicillins in aqueous electrolyte solution: a light-scattering and NMR study. Langmuir. 1999;15:2022–8.
4. Fini A, Fazio G, Feroci G. Solubility and solubilization properties of non-esteroidal anti-inflammatory drugs. Int J Pharm. 1995;126:95–102.
5. Taboada P, Attwood D, Ruso JM, García M, Mosquera V. Thermodynamic properties of some antidepressant drugs in aqueous solution. Langmuir. 2001;17:173–7.
6. Attwood D, Mosquera V, Lopez-Fontan JL, Garcia M, Sarmiento F. Self-association of phenothiazine drugs: influence of the counterion on the mode of association. J Colloid Interface Sci. 1996;184:658–62.
7. Frenkel YV, Clark AD, Das Jr K, Wang Y-H, Lewi PJ, Janssen PAJ, *et al.* Concentration and pH dependent aggregation of hydrophobic drug molecules and relevance to oral bioavailability. J Med Chem. 2005;48:1974–83.
8. Fernandez DA, Awruch J, Dicelio LE. Synthesis and photophysical properties of a new cationic water-soluble Zn phthalocyanine. J Photochem Photobiol B. 1997;41:227–32.
9. López-Nicolás JM, García-Carmona F. Effect of hydroxypropyl-β-cyclodextrin on the aggregation of (E)-resveratrol in different protonation states of the guest molecule. Food Chem. 2010;118:648–55.
10. Atwood D, Boitard E, Dubés J-P, Tachoire H. A colorimetric study of the influence of temperature on the self-association of amphiphilic antidepressant drugs in aqueous solution. J Colloid Interface Sci. 2000;227:356–62.
11. Domagk G, Behnisch R, Mietzsch F, Schimidt H. On a new class of compounds effective *in vitro* against tubercle bacilli. Naturwis. 1946;33:315.
12. Iakovidou Z, Papageorgiou A, Demertzis MA, Mioglou E, Mourelatos D, Kotsis A, *et al.* Platinum (II) and Palladium (II) complexes with 2-acetylpyridine thiosemicarbazone: cytogenetic and antineoplastic effects. Anti-Cancer Drugs. 2001;12:65–70.
13. Sriram D, Yogeeswari P, Dhakla P, Senthilkumar P, Banerjee D. N-Hydroxythiosemicarbazones: synthesis and *in vitro* antitubercular activity. Bioorg Med Chem Lett. 2007;17:1888–91.
14. Halve AK, Bhashkar B, Sharma V, Bhadauria R, Kankoriya A, Soni A, *et al.* Synthesis and *in vitro* antimicrobial studies of some new 3-[phenyldiazenyl] benzaldehyde *N*-phenyl thiosemicarbazones. J Enzyme Inhib Med Chem. 2008;23:77–81.
15. Du X, Guo C, Hansell E, Doyle PS, Caffrey CR, Holler TP, *et al.* Synthesis and structure–activity relationship study of potent trypanocidal thio semicarbazone inhibitors of the trypanosomal cysteine protease cruzain. J Med Chem. 2002;45:2695–707.
16. Pelosi G, Bisceglie F, Bignami F, Ronzi P, Schiavone P, Re MC, *et al.* Antiretroviral activity of thiosemicarbazone metal complexes. J Med Chem. 2010;53:8765–9.
17. Finkielstein LM, Castro E, Fabián LE, Moltrasio GY, Campos RH, Cavallaro LV, *et al.* New-1-indanone thiosemicarbazone derivatives active against BVDV. Eur J Med Chem. 2008;43:1767–73.
18. Brousse BN, Massa R, Moglioni AG, Martins Alho M, D'Accorso N, Gutkind G, *et al.* Antibacterial and antifungal activity of some thiosemicarbazones and 1,3,4-thiadiazolines. J Chil Chem Soc. 2004;49:45–9.
19. Garcia C, Brousse B, Carlucci M, Moglioni A, Martins Alho M, Moltrasio G, *et al.* Inhibitory effect of thiosemicarbazone derivatives on Junin virus replication *in vitro*. Antivir Chem Chemother. 2003;14:99–105.
20. Finkielsztein LM, Moltrasio GY, Caputto ME, Castro EF, Cavallaro LV, Moglioni AG. What is known about the antiviral agents active against Bovine Viral Diarrhea Virus (BVDV)? Curr Med Chem. 2010;17:2933–55.
21. Glisoni RJ, Chiappetta DA, Finkielsztein LM, Moglioni AG, Sosnik A. Self-aggregation behaviour of novel thiosemicarbazone drug candidates with potential antiviral activity. New J Chem. 2010;34:2047–58.
22. Brewster M, Loftsson T. Cyclodextrins as pharmaceutical solubilizers. Adv Drug Del Rev. 2007;59:645–66.

23. Loftsson T, Brewster M. Pharmaceutical Applications of Cyclodextrins. 1. Drug Solubilization and Stabilization. J Pharm Sci. 1996;85:1017–25.
24. Loftsson T, Másson M, Brewster ME. Self-association of cyclodextrins and cyclodextrin complexes. J Pharm Sci. 2004;93:1091–9.
25. Loftsson T, Duchêne D. Cyclodextrins and their pharmaceutical applications. Int J Pharm. 2007;329:1–11.
26. Zouvelekis D, Yannakopoulou K, Mavridis IM, Antoniadou-Vyza E. The self-association of the drug acemetacin and its interactions and stabilization with β-cyclodextrin in aqueous solution as inferred from NMR spectroscopy and HPLC studies. Carbohydrate Res. 2002;337:1387–95.
27. McIntosh MP, Leong N, Katneni K, Morizzi J, Shackleford DM, Prankerd RJ. Impact of chlorpromazine self-association on its apparent binding constants with cyclodextrins: effect of SBE7-β-CD on the disposition of chlorpromazine in the rat. J Pharm Sci. 2010;99:2999–3008.
28. Bonini M, Rossi S, Karlsson G, Almgren M, Lo Nostro P, Baglioni P. Self-assembly of β-Cyclodextrin in water. Part 1: Cryo-TEM and dynamic light scattering. Langmuir. 2006;22:1478–84.
29. He Y, Shen PFX, Gao H. Cyclodextrin-based aggregates and characterization by microscopy. Micron. 2008;39:495–516.
30. Messner M, Kurlov SV, Jansook P, Loftsson T. Self-assembled cyclodextrin aggregates and nanoparticles. Int J Pharm. 2009;387:199–208.
31. Szente L, Szejtli J, Kis GL. Spontaneous opalescence of aqueous γ-cyclodextrin solutions: complex formation or self-aggregation? J Pharm Sci. 1998;87:778–81.
32. Jansook P, Moya-Ortega MD, Loftsson T. Effect of self-aggregation of γ-cyclodextrin on drug solubilization. J Incl Phenom Macrocycl Chem. 2010;68:229–36.
33. Surfactant micelle characterization using dynamic light scattering. Malvern Instruments. Application Note. (2006).
34. Martin Del Valle EM. Cyclodextrins and their uses: a review. Proc Biochem. 2004;39:1033–46.
35. Higuchi T, Connors KA. Phase-solubillity techniques. Adv Anal Chem Instrum. 1965;4:117–212.
36. Jansook P, Kurkov SV, Loftsson T. Cyclodextrins as solubilizers: formation of complex aggregates. J Pharm Sci. 2010;99:719–29.
37. Garnero C, Zoppi A, Genovese D, Longhi M. Studies on trimethoprim: hydroxypropyl-β-cyclodextrin: aggregate and complex formation. Carbohydrate Res. 2010;345:2550–6.
38. Grant DJW, Higuchi T. Solubility Behavior of Organic Compounds. Techniques of Chemistry Volume XXI. Chapter 10. Wiley Interscience (1990).
39. European Pharmacopeia, 3rd Ed., Supplement 5.4. (Residual solvents), Page 298 (2000).
40. Mukne AP, Nagarsenker MS. Triamterene-β-cyclodextrin system: preparation, characterization and *in vivo* evaluation. AAPS PharmSciTech. 2004;5:1–9.
41. Kim Y-T, Shin B-K, Garripelli VK, Kim J-K, Davaa E, Jo S, *et al.* A thermosensitive vaginal gel formulation with HPγCD for the pH-dependent release and solubilization of amphotericin B. Eur J Pharm Sci. 2010;41:399–406.
42. Smith AA, Manavalan R, Kannan K, Rajendiran N. Spectral characteristics of tramadol in different solvents and β-cyclodextrin. Spectrochim Acta Part A. 2009;74:469–77.
43. Skiba M, Duchêne D, Puisieux F, Wouessidjewe D. Development of a new colloidal drug carrier from chemically-modified cyclodextrins: nanospheres and influence of physicochemical and technological factors on particle size. Int J Pharm. 1996;129:113–21.
44. Da Silveira AM, Ponchel G, Puisieux F, Duchêne D. Combined poly(isobutylcyanoacrylate) and cyclodextrins nanoparticles for enhancing the encapsulation of lipophilic drugs. Pharm Res. 1998;15:1051–5.
45. Choi M-J, Scoottitantawat A, Nuchuchua O, Min S-G, Ruktanonchai U. Physical and light oxidative properties of eugenol encapsulated by molecular inclusion and emulsion-diffusion method. Food Res Int. 2009;42:148–56.
46. Gould S, Scott R. 2-Hydroxypropyl-β-cyclodextrin (HPβ-CD): a toxicology review. Food Chem Toxicol. 2005;43:1451–9.
47. Li J, Zhang M, Chao J, Shuang S. Preparation and characterization of the inclusion complex of Baicalin (BG) with β-CD and HP-β-CD in solution: an antioxidant ability study. Spectrochim Acta Part A. 2009;73:752–6.
48. Yavuz B, Bilensoy E, Vural I, Şumnu M. Alternative oral exemestane formulation: improved dissolution and permeation. Int J Pharm. 2010;398:137–45.
49. Dupuy N, Barbry D, Bria M, Marquis S, Vrielynck L, Kister J. ^{1}H-NMR study of inclusion compounds of phenylurea derivatives in β-cyclodextrin. Spectrochim Acta Part A. 2005;61:1051–7.
50. Gibaud S, Zirar SB, Mutzenhardt P, Fries I, Astier A. Melarsoprol-cyclodextrins inclusion complexes. Int J Pharm. 2005;306:107–21.